J Physiol 587.24 (2009) pp 5843–5857

The Journal of Physiology

Differential induction of bidirectional long-term changes in neurotransmitter release by frequency-coded patterns at the cerebellar input

Anna D'Errico[1,4], Francesca Prestori[1,2] and Egidio D'Angelo[1,3]

[1] *Department of Physiology, University of Pavia, Via Forlanini 6, I-27100 Pavia, Italy*
[2] *Consorzio Interuniversitario per le Scienze Fisiche della Materia (CNISM), Via Bassi 6, I-27100 Pavia, Italy*
[3] *Brain Connectivity Center, Istituto Neurologico IRCCS fondazione C. Mondino, Via Mondino 2, I-27100 Pavia, Italy*
[4] *SISSA (International School for Advanced Studies), Neurobiology Sector, Trieste, Italy*

Sensory stimulation conveys spike discharges of variable frequency and duration along the mossy fibres of cerebellum raising the question of whether and how these patterns determine plastic changes at the mossy fibre–granule cell synapse. Although various combinations of high-frequency bursts and membrane depolarization can induce NMDA receptor-dependent long-term depression (LTD) and long-term potentiation (LTP), the effect of different discharge frequencies remained unknown. Here we show that low-frequency mossy fibre stimulation (100 impulses−1 Hz) induces mGlu receptor-dependent LTD. For various burst frequencies, the plasticity–$[Ca^{2+}]_i$ relationship was U-shaped resembling the Bienenstok–Cooper–Munro (BCM) learning rule. Moreover, LTD expression was associated with increased paired-pulse ratio, coefficient of variation and failure rate, and with a decrease in release probability, therefore showing changes opposite to those characterizing LTP. The plasticity–$[Ca^{2+}]_i$ relationship and the changes in neurotransmitter release measured by varying induction frequencies were indistinguishable from those obtained by varying high-frequency burst duration. These results suggest that different glutamate receptors converge onto a final common mechanism translating the frequency and duration of mossy fibre discharges into a regulation of the LTP/LTD balance, which may play an important role in adapting spatio-temporal signal transformations at the cerebellar input stage.

(Received 21 June 2009; accepted after revision 23 October 2009; first published online 26 October 2009)
Corresponding author E. D'Angelo: Universitá di Pavia, Istituto di Fisiologia Generale, Via Forlanini 6, Pavia I-27100, Italy. Email: dangelo@unipv.it

Abbreviations AIDA, (*RS*)-1-aminoindan-1,5-dicarboxylic acid; BCM, Bienenstok–Cooper–Munro; CAMKII, Ca^{2+}–calmodulin-dependent protein kinase II; CV, coefficient of variation; APV, (D)-(−)-2-amino-5-phosphonopentanoic acid; FR, failure rate; hfs, high-frequency stimulation; lfs, low-frequency stimulation; LTD, long-term depression; LTP, long-term potentiation; mGlu receptor, metabotropic glutamate receptor; OG1, Oregon Green BAPTA-1; PPR, paired-pulse ratio; ROI, region of interest.

Introduction

Long-term synaptic plasticity, a leading candidate for learning and memory in the brain (Bliss *et al.* 2003), is manifest through persistent change in synaptic transmission called long-term potentiation (LTP; Bliss & Collingridge, 1993) and long-term depression (LTD; Bear & Abraham, 1996). According to the Hebb postulate (Hebb, 1949) and its extension in the Bienenstock–Cooper–Munro model (BCM; Bienenstock *et al.* 1982), LTP and LTD are differentially induced depending on the pre- and postsynaptic activity patterns (Artola & Singer, 1993; Hansel *et al.* 1997; Cormier *et al.* 2001). Several experimental proofs have shown that the consequent postsynaptic $[Ca^{2+}]$ elevations (Lisman, 1989, 2001, 2003; Linden, 1999; Yang *et al.* 1999; Zucker, 1999; Augustine *et al.* 2003) regulate a bidirectional expression mechanism, being either a change in neurotransmitter release or in postsynaptic responsiveness. However, specific stimulus patterns can activate multiple mechanisms of plasticity at different synapses on the same neuron or even in the same synapse, with major

DOI: 10.1113/jphysiol.2009.177162

distinctions being based on the locus of induction and expression (pre- or postsynaptic) and on the alternate involvement of either NMDA or metabotropic glutamate (mGlu) receptors (for reviews, see Malenka & Nicoll, 1999; Anwyl, 2006; Letzkus *et al.* 2006).

The mossy fibre–granule cell relay of cerebellum raises an interesting case for several reasons. First, the granule cell has a simple structure, with a single synapse on each one of its four short and unbranched dendrites (Eccles *et al.* 1967). Secondly, the foundations of mossy fibre–granule cell synaptic transmission have been analysed in detail (D'Angelo *et al.* 1995; Silver *et al.* 1996; Sola *et al.* 2004; Saviane & Silver, 2006). Thirdly, the native mossy fibre input patterns are well known, being characterized either by short high-frequency bursts or by protracted frequency-modulated discharges depending on the nature of the stimulus (Kase *et al.* 1980; van Kan *et al.* 1993; Chadderton *et al.* 2004; Jörntell & Ekerot, 2006; Rancz *et al.* 2007; Arenz *et al.* 2008). Finally, it has recently been shown that, when high-frequency discharge exceeds a certain duration, mossy fibre–granule cell LTP is induced in an NMDA receptor-dependent manner (D'Angelo *et al.* 1999; Armano *et al.* 2000; Hansel *et al.* 2001; D'Angelo & DeZeeuw, 2009) through an increase in postsynaptic $[Ca^{2+}]_i$ (Gall *et al.* 2005) and is expressed through an increased neurotransmitter release probability (Sola *et al.* 2004; Nieus *et al.* 2006). The inhibitory regulation of membrane depolarization exerted by Golgi cells both *in vitro* (Mapelli & D'Angelo, 2007) and *in vivo* (Roggeri *et al.* 2008) can turn LTP into LTD. However, it is unknown whether LTP and LTD are regulated by frequency-coded patterns.

In this paper we show that long-term synaptic plasticity at the mossy fibre–granule cell synapse can be modulated by the frequency of stimulation through postsynaptic $[Ca^{2+}]_i$ elevations leading to a bidirectional regulation of neurotransmitter release. The plasticity–$[Ca^{2+}]_i$ relationship and expression mechanisms were similar to those determined by high-frequency bursts of various duration, except that low-frequency LTD required mGlu rather than NMDA receptors. This suggests that differential receptor pathways activated by a wide range of afferent patterns converge onto a common plastic mechanism providing the basis for adaptable reconfiguration of granular layer activity.

Methods

Ethical approval

The experiments reported in this paper have been conducted on 18- to 22-day-old (P0 = day of birth) Wistar rats ($n = 44$) according to protocols approved by the local ethical committee and by the European Commission (under the project SENSOPAC). All experimental procedures meet the guidelines set out in *The Journal of Physiology* for ethical matters (Drummond, 2009). The rats were anaesthetized with halothane (0.5 ml in 2 l administered for 1–2 min; Sigma, St Louis, MO, USA) and killed by decapitation in order to remove the cerebellum for acute slice preparation according to a well-established technique (D'Angelo *et al.* 1995, 1999; Armano *et al.* 2000; Sola *et al.* 2004; Gall *et al.* 2005; Forti *et al.* 2006).

Slice preparation and solutions

The cerebellar vermis was isolated and fixed on the vibroslicer's stage (Dosaka, Kyoto, Japan) with cyano-acrylic glue. Acute 220 μm-thick slices were cut in the parasagittal plane in cold cutting solution containing (in mM): 130 potassium gluconate, 15 KCl, 0.2 EGTA, 20 Hepes and 10 glucose, pH adjusted to 7.4 with NaOH. Slices were incubated for at least 1 h at room temperature (24–25°C) in oxygenated extracellular Krebs solution containing the following (in mM): 120 NaCl, 2 KCl, 2 $CaCl_2$, 1.2 $MgSO_4$, 1.2 KH_2PO_4, 26 $NaHCO_3$, 11 glucose, pH 7.4, when equilibrated with 95% O_2 and 5% CO_2. Slices were later transferred to a recording chamber mounted on the stage of an upright microscope (Zeiss, Oberkochen, Germany) and perfused (1–1.5 ml min^{-1}) with the same extracellular solution added with 10 μM bicuculline to block $GABA_A$ receptors (Biomol International, Pennsylvania, USA). Patch pipettes were pulled from borosilicate glass capillaries (Hilgenberg, Malsfeld, Germany) and, when filled with the intracellular solution, had a resistance of 7–9 MΩ before seal formation. The whole-cell recording pipettes were filled with the following solution (in mM): 126 potassium gluconate, 4 NaCl, 5 Hepes, 15 glucose, 1 $MgSO_4.7H_2O$, 0.1 BAPTA-free, 0.05 BAPTA-Ca^{2+}, 3 Mg^{2+}-ATP, 0.1 Na^+-GTP, pH 7.2 adjusted with KOH. This solution maintained resting free- $[Ca^{2+}]$ at 100 nM. In some experiments BAPTA was increased to 10 mM. (*RS*)-1-Aminoindan-1,5-dicarboxylic acid (AIDA; Tocris Bioscience) at 15 μM and (D)-(−)-2-amino-5-phosphonopentanoic acid (APV; Tocris Bioscience) at 100 μM were perfused locally through a multibarrel pipette.

Electrophysiological recordings

Whole-cell recordings were made with an Axopatch-200B (or Multiclamp 700B) amplifier (Molecular Devices, Union City, CA, USA) at room temperature (20–23°C), except for key recordings that were repeated at 34°C. Membrane current and potential were recorded using the voltage-clamp mode and the fast current-clamp mode of the amplifier, respectively (D'Angelo *et al.* 1995). All recordings were made at a cut-off frequency of 10 kHz and subsequently digitized at 20 kHz using pCLAMP 9

(Molecular Devices) in combination with a Digidata 1200B (or 1322A) A/D converter (Molecular Devices). Just after obtaining the cell-attached configuration, electrode capacitive transients were carefully cancelled to allow for electronic compensation of pipette charging during subsequent current-clamp recordings (D'Angelo *et al.* 1995, 1998).

The mossy fibre bundle was stimulated with a bipolar tungsten electrode (Clark Instruments, Pangbourne, UK) via a stimulus isolation unit using 200 μs pulses at a test frequency of 0.33 Hz (in specific experiments, paired-pulse stimulation at 20 ms inter-pulse intervals was used). From a comparison with data reported by Sola *et al.* (2004), between 1 and 2 mossy fibres were stimulated per granule cell. After evoking EPSCs at −70 mV at the test frequency for 10 min (control period), the recording was switched to current clamp. Synaptic plasticity was induced from a membrane potential around −50 mV by 100 stimuli at the frequencies of (in different experiments): 1, 8, 50 and 100 Hz. Then, after re-establishing voltage clamp at −70 mV, stimulation was restarted at the test frequency. EPSCs were digitally filtered at 1.5 kHz and analysed off-line with Clampfit 9 (Molecular Devices).

The stability of recordings can be influenced by modification of series resistance (R_s) and neurotransmitter release. This is a particularly important issue in evaluating LTD, since R_s most commonly tends to deteriorate with time potentially leading to spurious reduction in the fast EPSCs of the granule cell. To ensure that R_s remained stable during recordings, passive electrode–cell parameters were monitored throughout the experiments. The granule cell behaves like a lumped electrotonic compartment and can therefore be treated as a simple resistive–capacitive system, from which relevant parameters can be extracted by analysing passive current relaxations induced by 10 mV hyperpolarizing steps from a holding potential of −70 mV (D'Angelo *et al.* 1995, 1999; Silver *et al.* 1996). The voltage-clamp time constant, τ_{vc}, was estimated from mono-exponential fitting to current transients elicited by voltage steps. The 3 dB cut-off frequency of the electrode–cell system was calculated as $f_{vc} = (2\pi \times \tau_{vc})^{-1} = 2.4 \pm 0.1$ kHz ($n = 44$). Membrane capacitance $C_m = 3.0 \pm 0.1$ pF ($n = 44$) was measured from the capacitive charge (the area underlying current transient), membrane resistance $R_m = 1.9 \pm 0.1$ GΩ ($n = 44$) was obtained from the steady-state current flow, also yielding series resistance $R_s = \tau_{vc}/C_m = 26.9 \pm 2.1$ MΩ ($n = 44$). These values did not significantly change after 30 min attesting recording stability.

Data are reported as mean ± S.E.M., statistical comparisons are done using unpaired Student's *t* test, Mann–Whitney and Wilcoxon *U* tests, and differences are considered statistically significant at $P < 0.05$.

EPSC measurements and quantal analysis

In voltage-clamp recordings at −70 mV, the fast component of mossy fibre–granule cell EPSCs is generated almost exclusively by activation of AMPA receptors (Silver *et al.* 1996; D'Angelo *et al.* 1999). EPSC amplitude was measured as the difference between EPSC peak and the current level just before stimulation (Nieus *et al.* 2006). In addition to the fast component (direct response; time-to-peak < 1.5 ms), the EPSCs included a minor slow component (indirect response) due to neurotransmitter spillover (Silver *et al.* 1996). Neurotransmission failures usually showed only the indirect component. A minority of failures (< 2%) without the slow component were considered stimulation failures and were discarded from analysis. The error introduced in amplitude measurement by the failures, which have non-zero amplitude due to the indirect response, was eliminated by setting the amplitude of the indirect responses to zero (Sola *et al.* 2004).

In order to investigate the expression mechanism of long-term synaptic plasticity over a heterogeneous data set including this and previous works (Sola *et al.* 2004; Gall *et al.* 2005), a simplified version of quantal analysis was performed by measuring the mean M and standard deviation S of EPSC amplitude. All measurements were performed over $N = 100$ contiguous EPSCs minimizing errors introduced by small samples (data not shown). EPSC changes, which do not strictly require that single synaptic connections are isolated, were obtained from M and S:

the coefficient of variation,

$$\mathrm{CV} = S/M, \tag{1}$$

the number of failures,

$$\mathrm{FR} = N_0/N, \tag{2}$$

where N_0 is the number of null responses,

the paired-pulse ratio,

$$\mathrm{PPR} = M_2/M_1, \tag{3}$$

i.e. the ratio between the second and first EPSC amplitude in a doublet at 20 ms inter-pulse interval.

In general, one should expect that both FR, CV and PPR will increase (decrease) with a presynaptic LTD (LTP) expression, but would not change with a postsynaptic LTD (LTP) expression. The comparison between M and CV obtained before (state A) and after (state B) the induction of plasticity could be performed in the plot $(\mathrm{CV_B}/\mathrm{CV_A})^{-2}$ *vs.* M_B/M_A (Bekkers & Stevens, 1990; Malinow & Tsien, 1990; Sola *et al.* 2004). Assuming binomial statistics, this plot has the property that the unitary slope diagonal separates points caused by changes in quantum content ($m = np$, with n being the number of releasing sites and p the release probability) from those caused by changes in quantum size (q). In the LTP region ($M_B/M_A > 1$), points

caused by an increased quantum content lay above the diagonal, while those caused by increased quantum size lay below the diagonal. The opposite occurs in the LTD region ($M_B/M_A < 1$).

Selection of unitary connections, which were used for quantal parameter estimates, was performed following specific criteria previously validated at the mossy fibre–granule cell synapse. The mossy fibre–granule cell synapse is formed by just four connections per granule cell on average, which give rise to distinct step-like response amplitude levels by increasing stimulation intensity. In particular the sudden jump of responses from zero amplitude to an average size <35 pA (Sola *et al.* 2004; Saviane & Silver, 2006) was taken as an indication that the response involved a single synaptic contact (data not shown). Quantal analysis was then applied conforming to the methods previously developed for this same synapse (Sola *et al.* 2004; Saviane & Silver, 2006) and subsequently extended to the Golgi cell–granule cell synapse (Mapelli *et al.* 2009). According to these papers, the release process was approximated by a simple binomial model, $m = np$, and p was calculated as

$$p = 1 - \frac{M \times \mathrm{CV}^2}{q\,(1 + \mathrm{cv}^2)} \tag{4}$$

where q and cv^2 are the mean and variance of miniature synaptic currents (minis) ($q = 12.9$ and $\mathrm{cv}^2 = 0.123$ were taken from Sola *et al.* 2004; for additional information on these parameters see the references therein and in particular Silver *et al.* 1996, and Clements, 2003). In the cell sample used for this analysis, we measured $M = -34.8 \pm 2.6$ pA, $\mathrm{CV} = 0.38 \pm 0.03$, $p = 0.64 \pm 0.04$ and $n = 3.8 \pm 1.1$ ($n = 28$), supporting that a single synaptic contact was isolated in most cases (cf. Sola *et al.* 2004; Saviane & Silver, 2006). The error inherent in p and n estimates was calculated according to McLachlan (1978). The error arising from eqn (4) (3.5%) was small compared to the p change (13%). Alternative calculations done using the lower and upper limits of q reported for this synapse (10 pA < q < 14 pA) did not critically affect p and n estimates or the calculation of p changes.

Calcium imaging

Calcium imaging was performed as reported previously in this same preparation (Gall *et al.* 2005) by using Oregon green BAPTA-1 (OG1, Molecular Probes). Briefly, 0.2 mM OG1 was added to the intracellular solution by substitution in the BAPTA/Ca^{2+} buffer. Granule cells were identified with a × 63, 0.9 NA water immersion objective (Olympus, Hamburg, Germany). Digital fluorescence images were obtained using an excitation light source from T.I.L.L. Photonics (Planegg, Germany) controlled through Axon Imaging Workbench AIW5.2 (INDEC Systems). Images were acquired with a 50 ms exposure/image at video rate. Acquisition started after allowing > 2 min for dye loading in the neuron. After this time, the resting fluorescence (F_0) varied by less than 5% in each analysed cell region for the entire recording time and the background fluorescence (B_0) was also stationary. All stimulation protocols were separated by a minimum of 60 s in order to allow $[Ca^{2+}]_i$ to return to basal level. Cell damage was identified by the following signs: the failure of 200 ms depolarization at 0 mV in voltage clamp to elicit a fluorescence transient or the sudden inability of fluorescence levels to recover to baseline after stimulation. Such experiments were not analysed. We never observed bleaching of OG1 basal fluorescence during individual stimulations.

Stimulus-induced fluorescence changes were analysed off-line in the regions of interest (ROIs). For each experiment, regions were drawn by eye defining the ROIs in the first image of a sequence, thus giving a set of two-dimensional arrays of pixels. In addition, background fluorescence was evaluated by defining a background area of similar size close to the cell. For each ROI, a measurement of the relative change in fluorescence during cell stimulation, $\Delta F/F_0$ (F_0 is the mean resting fluorescence), was obtained as follows. (a) For each consecutive nth image in the sequence, the fluorescence intensity $f(n)$ was evaluated in the ROI. (b) Background fluorescence was measured simultaneously in the background area, $B(n)$. Care was taken to check that background fluorescence was stationary. (c) The background-subtracted fluorescence $F(n) = f(n) - B(n)$ was then used to evaluate

$$\Delta F/F_0(n) = (F(n) - F_0)/F_0, \tag{5}$$

where F_0 is the average background-subtracted resting fluorescence over four consecutive images before applying the stimulus. This background subtraction procedure was used to account for slice autofluorescence and/or fluorescence arising from outflow of dye from the pipette prior to seal formation. ROIs for analysis of somatic signals were chosen near the visible soma border to minimize the unfavourable surface/volume ratio for estimation of near-membrane Ca^{2+} changes. Analysis of images was performed with AIW-5.2 software.

It should be noted that intracellular buffers like BAPTA and OG1 have to be carefully calibrated in order to maintain efficient Ca^{2+} homeostasis and neuronal functional properties (D'Angelo *et al.* 1995). The BAPTA buffer, which has been extensively tested over the last few years in our laboratory, allows the induction of mossy fibre–granule cell long-term synaptic plasticity (D'Angelo *et al.* 1999; Rossi *et al.* 2002) with properties indistinguishable from those observed using perforated-patch or field recordings (Armano *et al.* 2000; Maffei *et al.* 2002). Moreover, granule cell intrinsic

excitability measured with BAPTA or in perforated-patch recordings is indistinguishable (Gall *et al.* 2003). OG1 has a Ca^{2+} affinity very similar to BAPTA therefore allowing a direct comparison of imaging with patch-clamp recordings. Indeed, the firing pattern observed using OG1 (see Fig. 1*B*) was indistinguishable from that observed using BAPTA (e.g. D'Angelo *et al.* 1995) and OG1 was not saturated by $[Ca^{2+}]_i$ changes (Gall *et al.* 2005). As well as in our previous work, $[Ca^{2+}]_i$ was measured in the granule cell dendritic ending showing the most prominent fluorescence change, in order to exclude non-synaptically activated dendrites, in which voltage-dependent calcium channels open due to electrotonic diffusion of depolarization.

Results

At the mossy fibre–granule cells synapse, LTP and LTD can be induced by high-frequency stimulus trains depending on the level of membrane depolarization, which is regulated by the local inhibitory circuit (D'Angelo *et al.* 1999; Armano *et al.* 2000; Mapelli & D'Angelo, 2007; Roggeri *et al.* 2008). The mechanism depends on voltage-dependent NMDA channel unblock (Gall *et al.* 2005). Indeed, 100 Hz–100 impulse trains from the holding potential of −50 mV induced LTP, while LTD was observed from lower holding potentials between −70 mV and −90 mV (Fig. 1*A*). Both early extracellular recordings (Kase *et al.* 1980; van Kan *et al.* 1993) and recent patch-clamp recordings (Chadderton *et al.* 2004; Rancz *et al.* 2007; Arenz *et al.* 2008) have revealed that mossy fibres convey either bursts or frequency-modulated discharges following sensory stimulation. In this study we have systematically investigated the relationship between the frequency of mossy fibre stimulation and synaptic plasticity. Moreover, we have addressed the hypothesis that a common mechanism of induction and expression governs LTP and LTD generated by combinations of burst frequency and duration through a comparison with previous data.

In order to normalize the induction protocols, a constant number of 100 stimuli was delivered while the frequency was varied between 1 Hz and 100 Hz. At 100 Hz–100 stimuli, this experimental series converges with that reported by Gall *et al.* (2005), who systematically changed burst duration from 10 ms to 1000 ms with

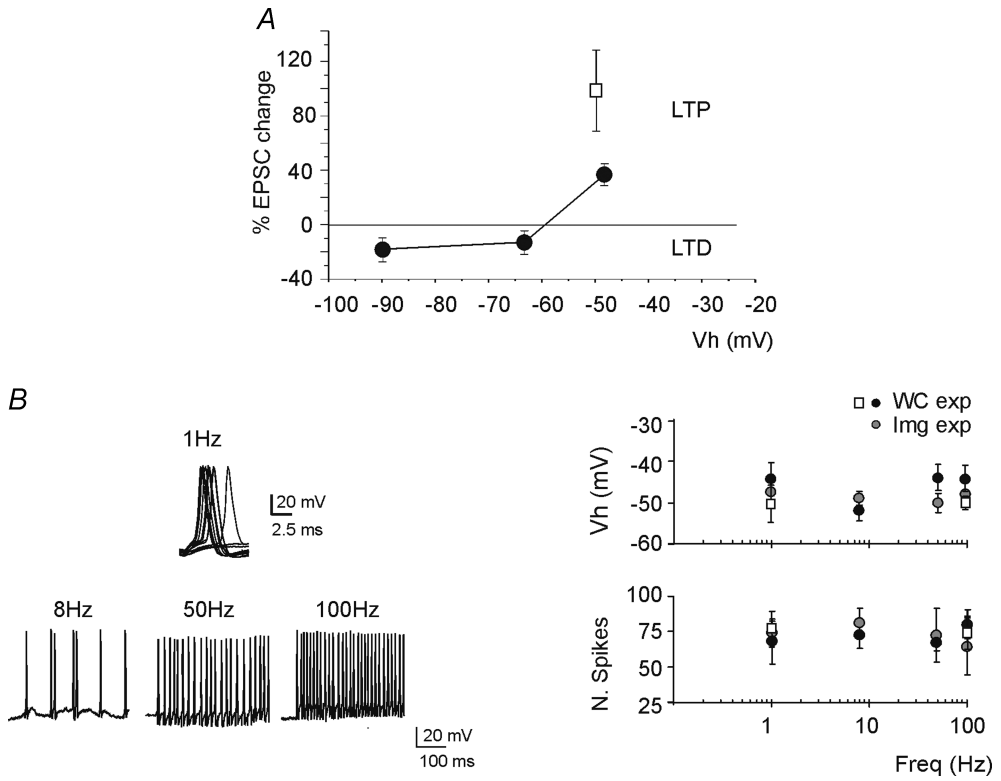

Figure 1. Bidirectional long-term synaptic plasticity: dependence on membrane potential
A, LTP or LTD were induced by applying the same stimulation protocol (100 impulses–100 Hz) from different holding potentials. *B*, sample traces have been taken during the induction protocol, demonstrating sustained firing at all induction frequencies. The plots show that the holding potential (V_h) before induction and the number of spikes elicited by the stimuli were similar at the different frequencies. The black circles represent experiments used for measuring the EPSCs (WC: whole-cell recording experiments; as in Fig. 2), the grey circles represent experiments used for calcium imaging (Img; as in Fig. 6), the white squares are obtained at 34°C. Data are reported as mean ± S.E.M.

a fixed frequency of 100 Hz. Moreover, in order to rule out the potential impact of membrane potential, the depolarization before delivery of induction trains was adjusted to around −50 mV. Neither the resting membrane potential prior to induction, nor the number of spikes elicited during induction (Linden, 1999), were substantially different while using different stimulation frequencies (Fig. 1*B*).

Frequency-modulated transition from LTD to LTP

Induction trains at different frequencies caused characteristic EPSC changes that persisted for the duration of recordings (Figs 2 and 3). At 1 Hz there was a high probability of observing LTD, with an EPSC average change of $-20.4 \pm 5.9\%$ ($n = 5$, $P < 0.05$). At 8 Hz the changes were scattered around the 0-level, with a nearly null average variation ($-1.9 \pm 7.2\%$; $n = 6$, $P = 0.9$). At 50 Hz there was a high probability of observing LTP, with an EPSC average change of $22.9 \pm 6.1\%$ ($n = 4$, $P < 0.005$). EPSC variations either in the LTP or LTD direction persisted until the end of recordings and were comparable in magnitude and time course to those reported in previous works (D'Angelo *et al.* 1999; Sola *et al.* 2004; Gall *et al.* 2005). This LTD obtained with low-frequency stimulation was dubbed lfs-LTD to be

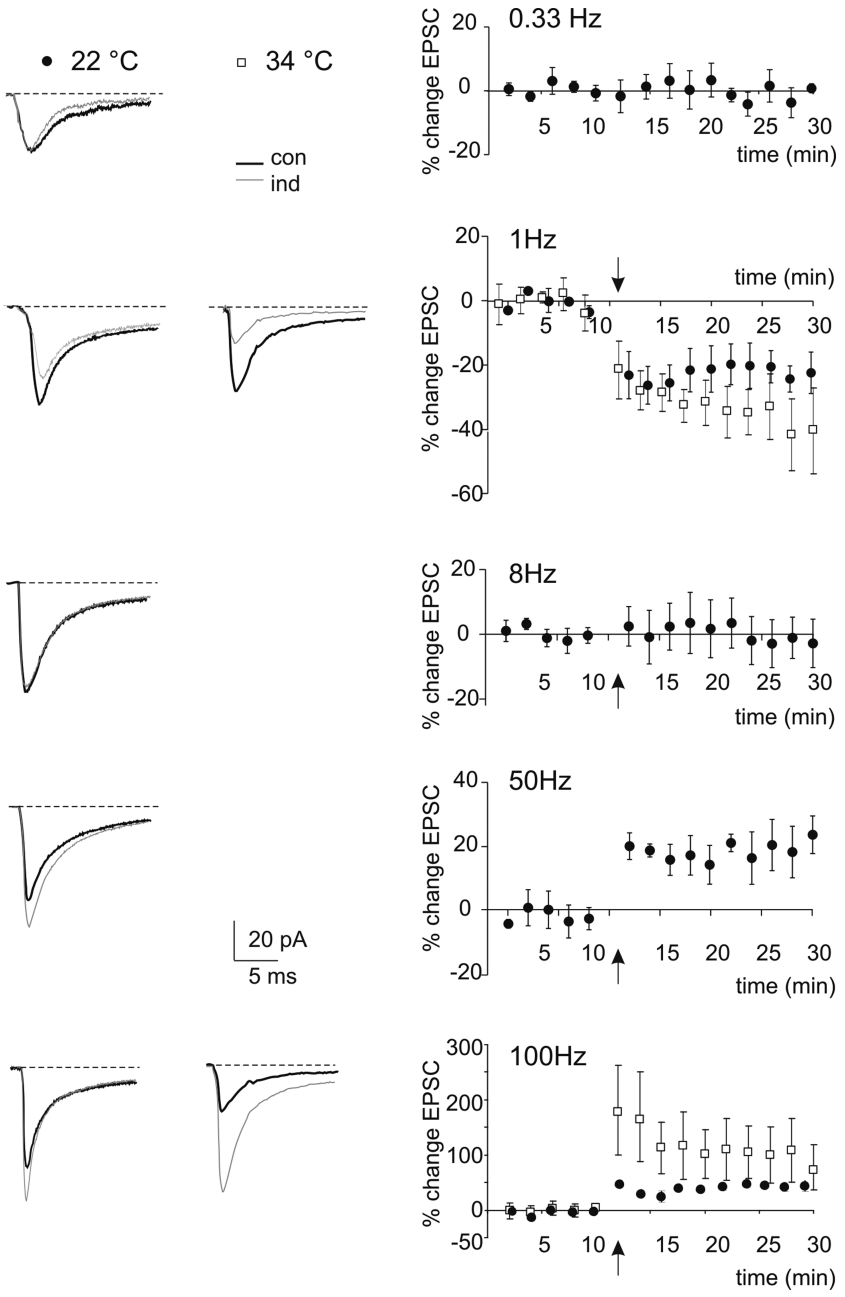

Figure 2. Bidirectional long-term synaptic plasticity induced by different stimulation frequencies
LTP or LTD were differentially induced by using the same number of impulses (100 impulses) at different frequencies. EPSC traces (average of 100 individual sweeps) illustrate the changes observed following induction in different experiments. The plots on the right show the average time course of changes at 0.1 Hz ($n = 6$), 1 Hz ($n = 5$), 8 Hz ($n = 6$), 50 Hz ($n = 4$) and 100 Hz ($n = 5$). For each series, data are expressed as percentage changes in EPSC peak amplitude compared to control (con) before induction (ind). The white squares represent data obtained at 34°C. The arrows indicate the induction time and each point is the average of 20 contiguous EPSC amplitudes. Data in the plots are reported as mean ± S.E.M.

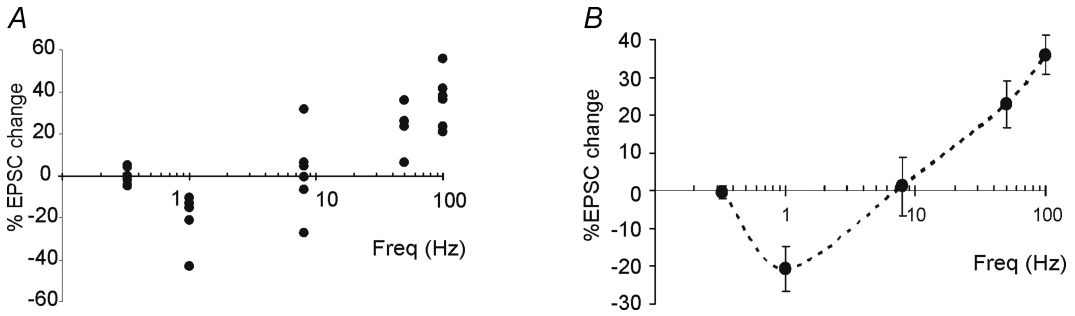

Figure 3. EPSC amplitude changes induced by different stimulation frequencies
A, the scatter plot on the left shows EPSC amplitude changes in individual recordings 15 min after induction (each point is the average of 100 EPSC amplitude measurements). The distribution of points reveals that the probability of obtaining LTD is high at 1 Hz, while that of obtaining LTP is high at 50 Hz, with a neutral point around 8 Hz. *B*, average EPSC amplitude changes in the same experiments as shown in *A* reveal a U-shaped relationship. Data in average plots are reported as mean ± S.E.M.

distinguished from that obtained using high-frequency stimulation at this same synapse (Gall *et al.* 2005) and dubbed hfs-LTD. LTP at 50 Hz, as well as LTP at 100 Hz in Gall *et al.* (2005), was dubbed hfs-LTP.

Since synaptic transmission and plasticity are temperature dependent, key recordings have been repeated at 34°C. Although robust demonstrations of mossy fibre–granule cell LTP were already obtained at 30–32°C (D'Angelo *et al.* 1999; Armano *et al.* 2000; Maffei *et al.* 2002, 2003; Sola *et al.* 2004; Mapelli & D'Angelo, 2007; Prestori *et al.* 2008), the presence and properties of LTD required to be confirmed. Indeed, several changes in synaptic excitation and plasticity have been reported with temperature (Klyachko & Stevens, 2006) although LTP induction was not much affected over 20°C (Krelstein *et al.* 1990; Andersen & Moser, 1995; Fujii *et al.* 2002). At 34°C, 100 Hz trains induced 100.6 ± 42.8% LTP ($n = 5$; $P < 0.05$) and 1 Hz trains induced −47.2 ± 7.9% LTD ($n = 6$; $P < 0.005$). Therefore, the basic pattern of changes analysed in this work was maintained, confirming the existence of LTP and LTD at the same synaptic relay observed *in vivo* at physiological temperature (Roggeri *et al.* 2008).

mGlu receptor-dependent induction of lfs-LTD

An intriguing aspect of lfs-LTD observed at hippocampal and neocortical synapses is that it can be generated by receptors and mechanisms partly differing from those of hfs-LTD. In some cases, lfs-LTD was shown to require mGlu rather than NMDA receptor activation, which are instead required for hfs-LTD (e.g. see Oliet *et al.* 1997; Nevian & Sackmann, 2006; Jo *et al.* 2008). Indeed, at the mossy fibre–granule cell synapse, hfs-LTD induced in the presence of strong synaptic inhibition is prevented by NMDA receptor antagonists (Mapelli & D'Angelo, 2007; Roggeri *et al.* 2008), but no information was available about lfs-LTD. Here, we show that the application of 15 μM AIDA (EPSC change = 5.1 ± 3.1; $n = 4$; $P = 0.7$) but not 100 μM APV (EPSC change = −27.4 ± 9.9; $n = 4$, $P < 0.05$) prevented the induction of lfs-LTD (Fig. 4), indicating that lfs-LTD at the mossy fibre–granule cell synapse of cerebellum requires mGlu receptor activation.

Calcium-dependent induction but presynaptic expression of lfs-LTD

The mechanisms of induction and expression of lfs-LTD were considered in detail by measuring EPSC fluctuations (CV), transmission failures (FR) and the paired-pulse ratio (PPR) (Fig. 5). CV, FR and PPR are informative about the

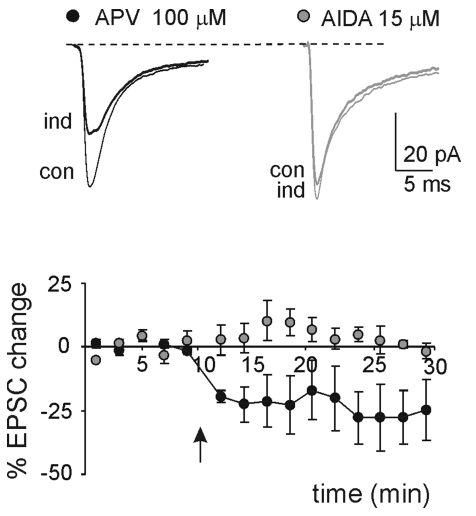

Figure 4. Postsynaptic mGlu receptor-dependent induction of lfs-LTD
Sample traces of EPSC in control (con) and 15 min after 1 Hz stimulation (ind) in a single cell (average of 100 sweeps) in presence of either 100 μM APV or 15 μM AIDA. The plot shows the time course of average EPSC amplitude changes (APV $n = 4$, AIDA $n = 4$). The arrows indicate the induction time and each point is the average of 20 contiguous EPSC amplitudes. Data are reported as mean ± S.E.M.

locus of neurotransmission changes. At the lfs-LTD steady state (15 min after induction, same cells as reported in Fig. 2 at 1 Hz), while the EPSC amplitude decreased, PPR increased by $23.8 \pm 7.6\%$ ($n = 5$, $P < 0.02$, paired t test), FR increased by $65.1 \pm 36.2\%$ ($n = 5$, $P < 0.05$, paired t test) and CV increased by $38.4 \pm 17.7\%$ ($n = 5$, $P < 0.05$, paired t test). These data suggest that a presynaptic change is at the origin of lfs-LTD. In a different series of recordings, in order to investigate whether lfs-LTD depended on postsynaptic Ca^{2+} concentration ($[Ca^{2+}]_i$) changes, the pipette intracellular solution was supplemented with 10 mM BAPTA. Figure 5 shows the time course of EPSC changes as well as of CV and PPR after a 1 Hz train. High BAPTA prevented lfs-LTD (EPSC amplitude $-3.8 \pm 3.9\%$, PPR $-4.2 \pm 3.4\%$, FR $-8.3 \pm 8.3\%$, CV $0.5 \pm 6.6\%$; $n = 4$ for all parameters, $P > 0.5$, paired t test). These results indicate, therefore, that lfs-LTD has postsynaptic calcium-dependent induction but presynaptic expression.

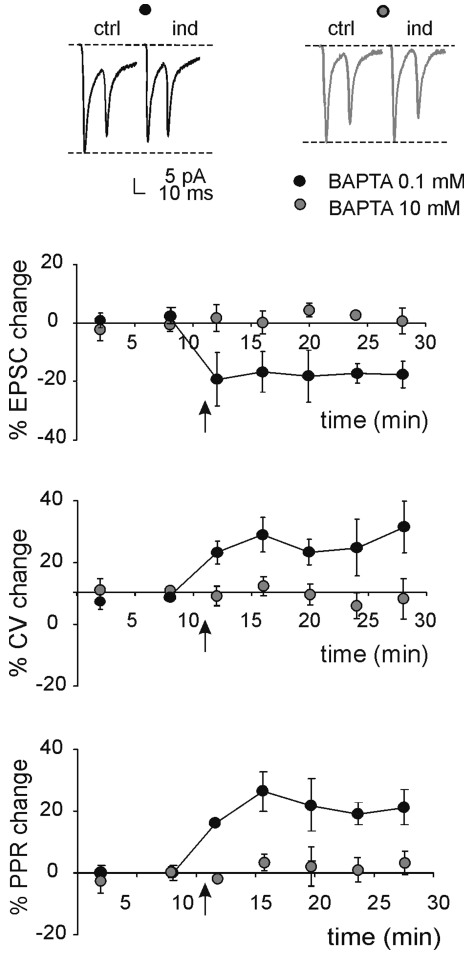

Figure 5. Postsynaptic Ca^{2+}-dependent induction but presynaptic expression of lfs-LTD
Sample traces of EPSC pairs in control (ctrl) and 15 min after 1 Hz stimulation (ind) in a single cell (average of 100 sweeps) either with 0.1 or 10 mM BAPTA in the intracellular solution.The reference lines indicate control EPSC amplitude. The plots show average changes in EPSC amplitude, CV and PPR after induction using either control ($n = 6$) or 10 mM BAPTA-containing intracellular solution ($n = 4$). The arrows indicate the induction time and each point is the average of 20 contiguous EPSC measurements. Data are reported as mean ± S.E.M.

Frequency dependence of intracellular Ca^{2+} changes

The relationship between intracellular calcium and stimulus frequency used for inducing long-term synaptic plasticity was investigated with Ca^{2+} imaging measurements using OG1 in the patch pipette (Fig. 6*A*; Gall *et al.* 2005). In order to obtain data comparable to those reported in Figs 1 and 2, induction was performed from an initial membrane potential of around −50 mV eliciting a number of spikes similar to that observed in the other plasticity experiments reported in the paper (cf. Fig. 1*B*). Application of 100 repetitive stimuli at frequencies between 1 and 100 Hz revealed, in the dendritic endings, a progressive $[Ca^{2+}]_i$ increase (Fig. 6*B*). There was a critical sensitivity of Ca^{2+} changes in the region of the LTP/LTD switch, while the $[Ca^{2+}]_i$ increase tended to a maximum level beyond 50 Hz (Fig. 6*C*). It should also be noted that the $[Ca^{2+}]_i$ increase became progressively slower as the induction frequency was reduced (Fig. 6*D*).

The BCM-like relationship between intracellular Ca^{2+} and synaptic plasticity

The relationship between synaptic plasticity and $[Ca^{2+}]_i$ (Fig. 7) showed a U-shape, with no plastic changes at very low $[Ca^{2+}]_i$, LTD for moderate $[Ca^{2+}]_i$ and, after a neutral point, LTP at relatively high $[Ca^{2+}]_i$. This relationship closely resembles that reported by using bursts of different duration (Gall *et al.* 2005), with the 100 Hz–100 ms points derived from the two experimental series being almost superimposed. Therefore, these results suggest that a postsynaptic mechanism based on the intensity of $[Ca^{2+}]_i$ change is responsible for both LTP and LTD induced by various frequency- and duration-modulated patterns. The two data sets proved to be statistically not dissimilar using the Wilcoxon–Mann–Whitney test (2 groups, $n = 5$ in each group, $P = 0.13$), and indicate that a common mechanism based on intracellular calcium changes can account for synaptic plasticity induced by a wide range of patterns at the mossy fibre–granule cell relay.

LTD and LTP as a bidirectional modulation of neurotransmitter release

The analysis of LTD and LTP expression was extended over the whole frequency range covered in these experiments. At all frequencies, the EPSC mean amplitude changes were

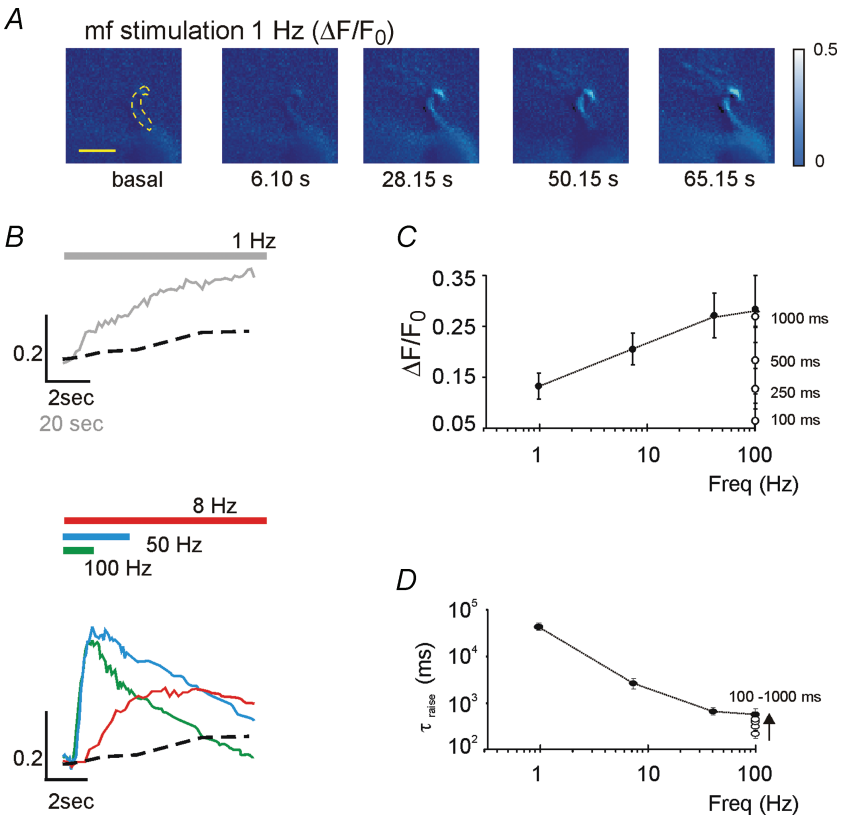

Figure 6. Intra-dendritic calcium changes induced by different stimulation frequencies
Analysis of $[Ca^{2+}]_i$ transients elicited by different mossy fiber (mf) stimulation frequencies in granule cells filled with 200 μM OG1. *A*, the series of pseudo-ratio images illustrates fluorescence changes $\Delta F/F_0$ at 1 Hz (the ROI used for measurements is indicated by a dashed line, scale bar = 5 μm; fluorescence intensity is colour-coded with arbitrary units). *B*, the traces show the background-subtracted kinetics of fluorescence changes, $\Delta F/F_0(n)$, for different stimulation frequencies (note different time scales at 1 Hz). The coloured bars indicate the duration of the stimulation trains. *C*, maximum $[Ca^{2+}]_i$ increase; and *D*, time-to-peak of the $[Ca^{2+}]_i$ increase during induction at different frequencies (1 Hz $n = 5$; 10 Hz $n = 8$; 50 Hz $n = 8$; 100 Hz $n = 6$; each cell contributes to at least three different frequencies). In both *C* and *D*, the white circles are data from Gall *et al.* (2005) at different burst durations but same 100 Hz frequency. Data are reported as mean ± S.E.M.

accompanied by symmetric CV variations, so that CV changes were usually positive for lfs-LTD and negative for hfs-LTP. These results were pooled together with those obtained using short and long 100 Hz trains in Gall *et al.* (2005). The ensemble CV–*M* plot for LTP and LTD obtained using patterns differing in either frequency or duration (Fig. 8*A*) showed a significant negative linear correlation passing near the origin ($R^2 = 0.52$, $n = 38$, $P < 0.0001$). Therefore, LTP and LTD changes caused by variation in burst frequency and duration appeared to exploit a common expression mechanism consisting of a bidirectional modulation of neurotransmitter release.

An additional method to determine whether EPSC changes depend on quantum content or quantum size is to plot $(CV_B/CV_A)^{-2}$ *vs.* M_B/M_A (Fig. 8*B*; Bekkers & Stevens, 1990; Malinow & Tsien, 1990; Sola *et al.* 2004), where A and B indicate the response before and after induction and CV and *M* have their usual meaning (coefficient of variation and mean amplitude, see Methods). The plot in Fig. 8*B* shows that most LTP and LTD points fall in the regions corresponding to changes in quantum content (above the unitary diagonal in the LTP region, below the diagonal in the LTD region). Taken together, the data in Fig. 8*A* and *B* suggest that LTD and LTP expression following bursts of different frequency and duration represent a continuum of changes depending on modulation of a common presynaptic mechanism. Quantal analysis was applied on a limited set of experiments, in which single-fibre

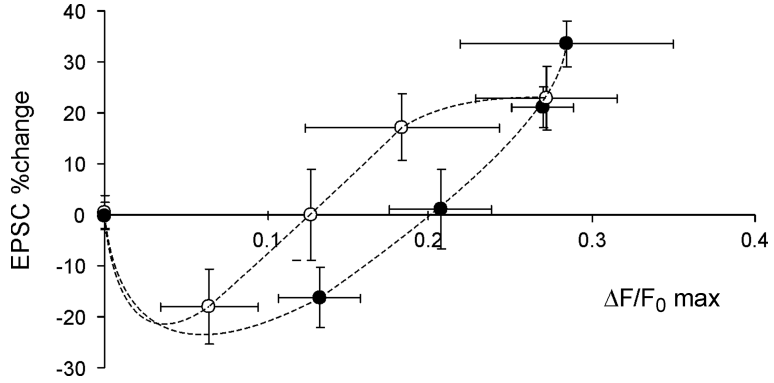

Figure 7. The relationship between intracellular calcium changes and synaptic plasticity
The relationship between intracellular calcium changes, $[Ca^{2+}]_i$, and synaptic plasticity obtained using different stimulation frequencies and durations (white circles are data from Gall *et al.* 2005). A dashed line is drawn through the points of each data set.

stimulation was most likely to having been achieved (Sola *et al.* 2004; Saviane & Silver, 2006; see Methods). In these connections, after induction at 1 Hz, release probability decreased by 13% ($n = 5$; $P < 0.05$), accounting for more than half of the average lfs-LTD.

Figure 9 summarizes the results of lfs-LTD and hfs-LTD expression and also shows those obtained by using long and short high-frequency stimulation trains causing hfs-LTP and hfs-LTD. In all cases, the same procedures for calculating PPR and release probability were applied. Concerning the changes in EPSC amplitude, CV, failure rate and release probability, the properties of lfs-LTD proved very similar to those of hfs-LTD but opposite to those of hfs-LTP. The differences between LTP and LTD were also maintained at 34°C indicating that the reported mechanisms could also operate at physiological temperature.

Discussion

In this paper we have identified a form of low-frequency LTD and analysed its properties together with those of plasticity induced by other activity patterns at the mossy fibre–granule cell synapse of cerebellum. We found that mGlu and NMDA receptors differentially control lfs-LTD and hfs-LTD/hfs-LTP, respectively. Nonetheless, burst patterns differing in either frequency or duration similarly modulate the LTP/LTD balance by controlling postsynaptic Ca^{2+} increase and by causing a bidirectional change in neurotransmitter release. Thus, a single mechanism activated through different glutamate receptors is sufficient to explain long-term synaptic plasticity caused by a broad range of input patterns. The changes in synaptic efficacy were also observed close to physiological body temperature and could explain LTP and

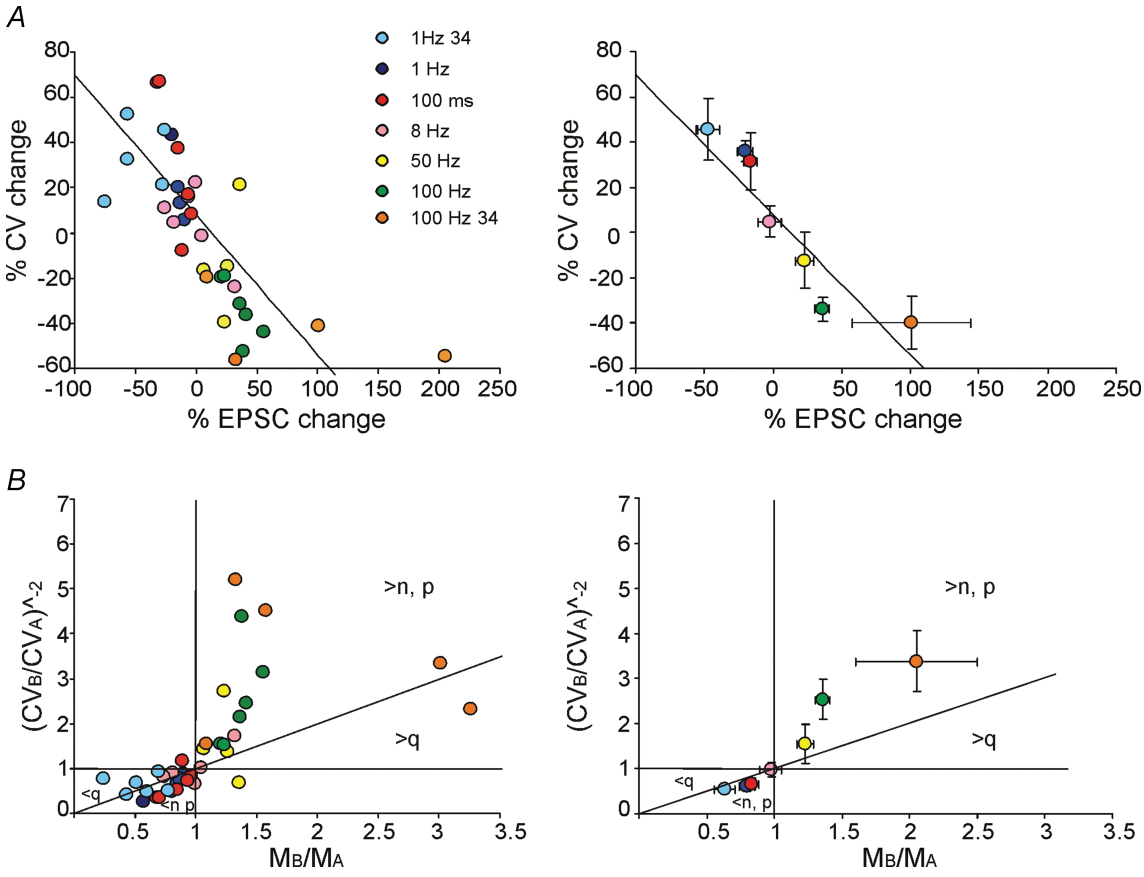

Figure 8. The relationship between CV and mean EPSC amplitude during LTP and LTD expression
The plots show data obtained at different frequencies (1, 8, 50 and 100 Hz; same as in Figs 2 and 3) and burst durations (10 impulse bursts at 100 Hz; from Gall *et al.* 2005). Data obtained at 24°C are also shown. Single data points (left plots) and average data grouped per category (right). *A*, the plots show the relationship between CV and EPSC changes at different frequencies. During LTP, EPSC CV decreased and EPSC amplitude increased, while the opposite occurred during LTD. Linear regression over the points was statistically significant (slope -0.62 ± 0.10, intercept 7.92 ± 4.9; $R^2 = 0.52$; $n = 38$; $P < 0.0001$). *B*, the plots $(CV_B/CV_A)^{-2}$ *vs.* M_B/M_A show that most LTP-related points fall in the regions of increased quantum content, i.e. above the unitary diagonal for $M_B/M_A > 1$, while most LTD-related points fall in the regions of decreased quantum content, i.e. below the unitary diagonal for $M_B/M_A < 1$. Data in average plots are reported as mean ± S.E.M.

LTD recently reported *in vivo* in the cerebellum granular layer (Roggeri *et al.* 2008).

LTP, LTD and the patterns of mossy fibre activity

As far as a sufficient number of impulses and membrane depolarization were provided, LTD was generated at 1 Hz and LTP at 50–100 Hz, while the probability of having one or the other became similar around 10 Hz determining the reversal point (a different kind of reversal was reported in hippocampal cells by Cho *et al.* 2001, in which no plasticity at all was observed). Moreover, low-frequency stimulation had nearly the same effect in determining LTD as short high-frequency bursts (Gall *et al.* 2005). The patterns to be transformed into LTP in the granular layer are therefore high-frequency (> 50 Hz) bursts lasting at least ∼100 ms. This matches the patterns generated by sensory stimuli, which consist of either 50–100 ms high-frequency bursts (with average frequency around 100 Hz and instantaneous frequencies up to 500–1000 Hz) or protracted frequency-modulated discharges (modulated from a few to over 50 Hz) (Eccles *et al.* 1967; Kase *et al.* 1980; van Kan *et al.* 1993; Chadderton *et al.* 2004; Jörntell & Ekerot, 2006; Rancz *et al.* 2007; Arenz *et al.* 2008). One possibility is therefore that mossy fibre–granule cell synapses are kept at relatively low efficiency (LTD) whenever background levels of activity (low-frequency or short occasional bursts) are prevalent, while transition to high efficiency levels (LTP) would occur following strong activity (high-frequency, long or repeated bursts). Coincidence detection in granule cells (D'Angelo *et al.* 1995; Jörntell & Ekerot, 2006) could bias the system toward LTP while synaptic inhibition provided by Golgi cells could bias the system toward LTD (Mapelli & D'Angelo, 2007). Thus, in line with the Hebb postulate, LTP is induced following intense (high-frequency and prolonged) co-activation of the pre- and postsynaptic neuron (Hebb, 1949). LTD, by being induced following weak (low-frequency and brief) co-activation of the pre- and postsynaptic neuron, conforms to an anti-hebbian rule.

Postsynaptic calcium-dependent induction but presynaptic expression

The induction mechanism, for all patterns investigated so far at the mossy fibre–granule cell synapse, was based on intracellular calcium changes occurring in the postsynaptic neuron. The frequency of stimulation regulated $[Ca^{2+}]_i$ increase, so that lower calcium levels caused LTD, intermediate levels were at the neutral point, and higher levels corresponded to LTP. This relationship was indistinguishable from the BCM-like relationship previously obtained using different burst durations (Gall *et al.* 2005), suggesting that the intracellular calcium level attained during a train is the critical element determining the sign of plasticity (Lisman, 2001, 2003; but see Nevian & Sackman, 2006). The time course of calcium changes, although varying over three orders of magnitude, did not prove to be critical. This observation prompts the identification of calcium-dependent processes, such as those based on the Ca^{2+}–calmodulin-dependent protein kinase II (CaMKII)/calcineurin balance and proposed for pyramidal neurons (Lisman, 2003), which could mediate the effect. At the present stage it was not possible to define whether a parallel or a serial reaction scheme activated by calcium would be better suited to explain the result.

The expression mechanism was almost entirely based on presynaptic changes in neurotransmitter release. The main arguments in favour of a presynaptic change during lfs-LTD, as well as the other forms of LTP and LTD observed at the mossy fibre–granule cell synapse of cerebellum, were the significant and persistent changes in CV, failures and PPR. CV was analysed in detail over the

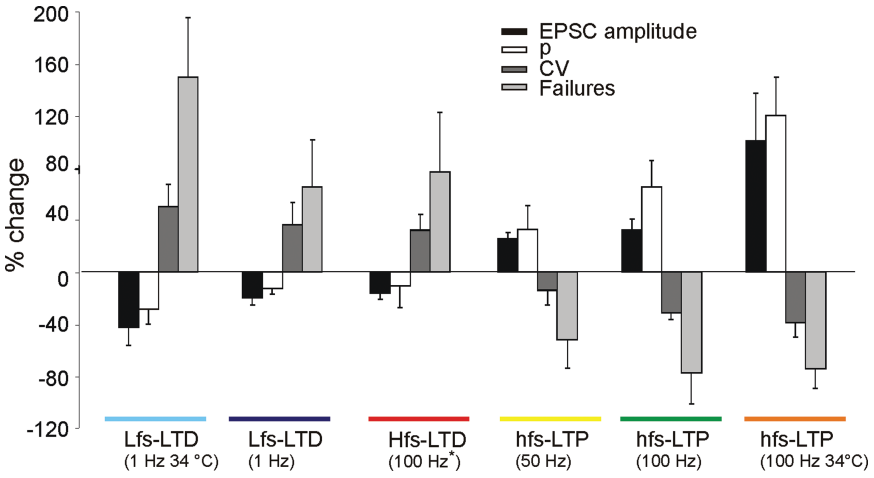

Figure 9. Summary of neurotransmission changes during LTD and LTP expression
The plot compares EPSC amplitude, CV and failure rate, and release probability (*p*) changes following different induction protocols comprising 1, 50 and 100 Hz trains with 100 impulses (same as in Fig. 8) as well as 100 Hz trains with 10 impulses. The hfs-LTD data are taken from Gall *et al.* (2005). Note that all the hfs-LTP (> 50 Hz) patterns are similar, as well as the lfs-LTD and hfs-LTD patterns of expression.

whole frequency range explored, showing a continuous variation with frequency. CV showed changes opposite to those of mean amplitude so that the relationship of the two variables was linear. Consistent with a presynaptic change, LTD points fell into the appropriate sector in the $(CV_B/CV_A)^{-2}$ *vs.* M_B/M_A plot (Bekkers & Stevens, 1990; Malinow & Tsien, 1990; Sola *et al.* 2004). The reduction in release probability estimated by CV/*M* analysis was 13%, sufficient to explain a large part of LTD at 1 Hz. Therefore, neurotransmitter release could be dynamically regulated by a bidirectional LTP/LTD switch controlled by postsynaptic induction, as originally reported at hippocampal synapses (e.g. see Dudek & Bear, 1993; Bolshakov & Siegelbaum, 1994), and implying the involvement of retrograde signalling. The presence of a minority of points in the $(CV_B/CV_A)^{-2}$ *vs.* M_B/M_A plot falling into the regions of increased quantum content suggested the coexistence of postsynaptic expression components (this case was indeed reported at hippocampal mossy fibre–interneuron synapses; Lei & McBain, 2004; Anwyl, 2006).

Transduction mechanisms: comparison with other synapses

While all forms of plasticity previously reported at the mossy fibre–granule cell synapse following high-frequency stimulation (both hfs-LTD and hfs-LTP) were fully prevented by NMDA receptor antagonists (D'Angelo *et al.* 1999; Armano *et al.* 2000; Mapelli & D'Angelo, 2007; Roggeri *et al.* 2008), lfs-LTD was prevented by blocking mGlu receptors, which, given the relative specificity of AIDA, were probably of type-1. In hfs-LTP (and possibly hfs-LTD) mGlu receptors showed a regulatory role but did not prove to be essential (D'Angelo *et al.* 1999; Maffei *et al.* 2002). This may reflect the prevalent engagement of the mGlu receptor-mediated pathway when stimulation frequency is low and temporal summation of NMDA receptor responses wanes (D'Angelo *et al.* 1995; J. Mapelli, D. Gandolfi & E. D'Angelo, unpublished observations). This hypothesis is in keeping with the moderate calcium increase determined by postsynaptic mGlu receptors in cerebellar granule cells (Gall *et al.* 2005). An mGlu receptor-dependent Ca^{2+} increase supported by Ca^{2+} stores has been observed in other neurons (Nishiyama *et al.* 2000; reviewed in Anwyl, 2006). It seems less likely that mGlu receptors were critical for regulating the sign of plasticity, since this was already determined by the $[Ca^{2+}]$ level, a variable controlled not only by mGlu but also by NMDA receptors. A critical role for mGlu receptors in plasticity switching was reported for spike-timing-dependent plasticity in layer II–IV pyramidal neurons (Nevian & Sackmann, 2006).

The induction mechanism of lfs-LTD at the mossy fibre–granule cells synapse, by strictly depending on mGlu receptors, is somehow simpler than at CA1 and perirhinal cortex synapses, where NMDA and mGlu receptor-dependent lfs-LTD coexist (see the original work of Mulkey & Malenka, 1992, and following on from this, Oliet *et al.* 1997; Jo *et al.* 2008). Interestingly, at CA1 synapses, NMDA receptor-dependent but not mGlu receptor-dependent lfs-LTD proved to be associated with the reduction of release from the rapidly recycling presynaptic vesicle pool (Stanton *et al.* 2003) through NO production and retrograde diffusion (Zhang *et al.* 2006). A different mechanism was reported at cortical afferents innervating the dorsolateral striatum, in which lfs-LTD proved to depend on postsynaptic release and retrodiffusion of endocannabinoids (Ronesi & Lovinger, 2005). The retrograde messenger of lfs-LTD and hfs-LTD at the mossy fibre–granule cell synapse is currently unknown (though hfs-LTP requires NO; Maffei *et al.* 2003). Finally, it should be noted that mGlu receptors and also $GABA_B$ receptors may take part in the induction process by regulating release probability, postsynaptic responsiveness and glomerular crosstalk (e.g. see Mitchell & Silver, 2000*a*,*b*; Mapelli *et al.* 2009). A further understanding of retrograde messengers and regulatory mechanisms opens interesting issues for future investigation.

Conclusions and functional implications

The mGlu receptors, by rendering induction mechanisms sensitive to low-frequency mossy fibre inputs, extend the physiological range over which granular layer LTP and LTD can take place. Stimuli characterized by spikes at low frequency, as well as by short spike bursts and unfavourable excitatory/inhibitory balance, may be regarded as 'irrelevant' and associated with LTD. Conversely, stimuli characterized by high-frequency protracted spike discharges and favourable excitatory/inhibitory balance may be regarded as 'relevant' and associated with LTP. The same mechanism could contribute to organizing the granular layer in centre–surround (Mapelli & D'Angelo, 2007): while stimuli generated at the centre of a sensory receptive field have burst-like properties causing LTP, those generated at the periphery have lower frequency causing LTD.

The impact of bidirectional long-term synaptic plasticity is better understood by considering responses to punctuate stimuli (Chadderton *et al.* 2004; Rancz *et al.* 2007), in which intense stimuli would elicit repeated high-frequency bursts and LTP, while weak stimuli would generate LTD. A specific issue arises with protracted stimuli causing alternating sequences of high and low frequency spike discharges, e.g. when eliciting the vestibulo-ocular reflex (see Arenz *et al.* 2008, for a recent report). It is currently unknown whether mossy fibre–granule cell LTP and LTD are mutually reversible

and how plasticity is established following such complex time-dependent patterns. Although several aspects remain to be determined, LTP and LTD have the potential of adapting spatio-temporal patterns transmitted through the mossy fibre pathway regulating the intensity, delay and extension of signals to be relayed to the molecular layer and Purkinje cells (D'Angelo & DeZeeuw, 2009).

References

Andersen P & Moser EI (1995). Brain temperature and hippocampal function. *Hippocampus* **5**, 491–498.

Anwyl R (2006). Induction and expression mechanisms of postsynaptic NMDA receptor-independent homosynaptic long-term depression. *Prog Neurobiol* **78**, 17–37.

Arenz A, Silver RA, Schaefer AT & Margrie TW (2008). The contribution of single synapses to sensory representation in vivo. *Science* **312**, 977–980.

Armano S, Rossi P, Taglietti V & D'Angelo E (2000). Long-term potentiation of intrinsic excitability at the mossy fibre–granule cell synapse of rat cerebellum. *J Neurosci* **20**, 5208–5216.

Artola A & Singer W (1993). Long-term depression of excitatory synaptic transmission and its relationship to long-term potentiation. *Trends Neurosci* **16**, 480–487.

Augustine GJ, Santamaria F & Tanaka K (2003). Local calcium signalling in neurons. *Neuron* **40**, 331–346.

Bear MF & Abraham WC (1996). Long-term depression in hippocampus. *Annu Rev Neurosci* **19**, 437–462.

Bienenstock EL, Cooper LN & Munro PW (1982). Theory for the development of neuron selectivity: orientation specificity and binocular interaction in visual cortex. *J Neurosci* **2**, 32–48.

Bliss TV & Collingridge GL (1993). A synaptic model of memory: long-term potentiation in the hippocampus. *Nature* **361**, 31–39.

Bliss TV, Collingridge GL & Morris RG (2003). Long-term potentiation and structure of the issue. *Philos Trans R Soc Lond B Biol Sci* **358**, 607–611.

Bolshakov VY & Siegelbaum SA (1994). Postsynaptic induction and presynaptic expression of hippocampal long-term depression. *Science* **264**, 1148–1152.

Bekkers JM & Stevens CF (1990). Presynaptic mechanism for long-term potentiation in the hippocampus. *Nature* **346**, 724–729.

Chadderton P, Margrie TW & Hausser M (2004). Integration of quanta in cerebellar granule cells during sensory processing. *Nature* **428**, 856–860.

Cho K, Aggleton JP, Brown MW & Bashir ZI (2001). An experimental test of the role of postsynaptic calcium levels in determining synaptic strength using perirhinal cortex of rat. *J Physiol* **532**, 459–466.

Clements JD (2003). Variance-mean analysis: a simple and reliable approach for investigating synaptic transmission and modulation. *J Neurosci Methods* **130**, 115–125.

Cormier RJ, Greenwood AC & Connor JA (2001). Bidirectional synaptic plasticity correlated with the magnitude of dendritic calcium transients above a threshold. *J Neurophysiol* **85**, 399–406.

D'Angelo E, De Filippi G, Rossi P & Taglietti V (1995). Synaptic excitation of individual rat cerebellar granule cells *in situ*: evidence for the role of NMDA receptors. *J Physiol* **484**, 397–413.

D'Angelo E & DeZeeuw CI (2009). Timing and plasticity in the cerebellum: focus on the granular layer. *Trends Neurosci* **32**, 30–40.

D'Angelo E, Rossi P, Armano S & Taglietti V (1999). Evidence for NMDA and mGlu receptor-dependent long-term potentiation of mossy fibre–granule cell transmission in rat cerebellum. *J Neurophysiol* **81**, 277–287.

Drummond GB (2009). Reporting ethical matters in *The Journal of Physiology*: standards and advice. *J Physiol* **587**, 713–719.

Dudek SM & Bear MF (1993). Bidirectional long-term modification of synaptic effectiveness in the adult and immature hippocampus. *J Neurosci* **13**, 2910–2918.

Eccles JC, Ito M & Szentagothai J (1967). *The Cerebellum as a Neuronal Machine*. Springer Verlag, Berlin, Germany.

Forti L, Cesana E, Mapelli J & D'Angelo E (2006). Ionic mechanism of autorhythmic firing in rat cerebellar Golgi cells. *J Physiol* **547**, 711–729.

Fujii S, Sasaki H, Ito K, Kaneko K & Kato H (2002). Temperature dependence of synaptic responses in guinea pig hippocampal CA1 neurons in vitro. *Cell Mol Neurobiol* **22**, 379–391.

Gall D, Prestori F, Sola E, D'Errico A, Roussel C, Forti L, Rossi P & D'Angelo E (2005). Intracellular calcium regulation by burst discharge determines bidirectional long-term synaptic plasticity at the cerebellum input stage. *J Neurosci* **25**, 4813–4822.

Gall D, Roussel C, Susa I, D'Angelo E, Rossi P, Bearzatto B, Galas MC, Blum D, Schurmans S & Schiffman SN (2003). Altered neuronal excitability in cerebellar granule cells of mice lacking calretinin. *J Neurosci* **23**, 9320–9327.

Hansel C, Artola A & Singer W (1997). Relation between dendritic Ca^{2+} levels and the polarity of synaptic long-term modifications in rat visual cortex neurons. *Eur J Neurosci* **9**, 2309–2322.

Hansel C, Linden DJ & D'Angelo E (2001). Beyond parallel fibre LTD: the diversity of synaptic and non-synaptic plasticity in the cerebellum. *Nat Neurosci* **4**, 467–475.

Hebb DO (1949). *The Organization of Behaviour*. Wiley, New York.

Jo J, Heon S, Kim MJ, Son GH, Park Y, Henley JM, Weiss JL, Sheng M, Collingridge GL & Cho K (2008). Metabotropic glutamate receptor-mediated LTD involves two interacting Ca^{2+} sensors, NCS-1 and PICK1. *Neuron* **60**, 1095–1111.

Kase M, Miller DC & Noda H (1980). Discharges of Purkinje cells and mossy fibres in the cerebellar vermis of the monkey during saccadic eye movements and fixation. *J Physiol* **300**, 539–555.

Klyachko VA & Stevens CF (2006). Temperature-dependent shift of balance among the components of short-term plasticity in hippocampal synapses. *J Neurosci* **26**, 6945–6957.

Krelstein MS, Thomas MP & Horowitz JM (1990). Thermal effects on long-term potentiation in the hamster hippocampus. *Brain Res* **520**, 115–122.

Jörntell H & Ekerot CF (2006). Properties of somatosensory synaptic integration in cerebellar granule cells in vivo. *J Neurosci* **26**, 11786–11797.

Lei S & McBain CJ (2004). Two loci of expression for long-term depression at hippocampal mossy fibre-interneuron synapses. *J Neurosci* **24**, 2112–2121.

Letzkus JJ, Kampa BM & Stuart GJ (2006). Learning rules for spike timing-dependent plasticity depend on dendritic synapse location. *J Neurosci* **26**, 10420–10429.

Linden DJ (1999). The return of the spike: postsynaptic action potentials and the induction of LTP and LTD. *Neuron* **22**, 661–666.

Lisman JE (1989). A mechanism for the Hebb and the anti-Hebb processes underlying learning and memory. *Proc Natl Acad Sci U S A* **86**, 9574–9578.

Lisman JE (2001). Three Ca^{2+} levels affect plasticity differently: the LTP zone, the LTD zone, and no man's land. *J Physiol* **532**, 285.

Lisman JE (2003). Long-term potentiation: outstanding questions and attempted synthesis. *Philos Trans R Soc Lond B Biol Sci* **358**, 829–842.

McLachlan EM (1978). The statistics of transmitter release at chemical synapses. In *International Review of Physiology. Neurophysiol III*, vol. 17, ed. Porter R. University Park Press, Baltimore.

Maffei A, Prestori F, Rossi P, Taglietti V & D'Angelo E (2002). Presynaptic current changes at the mossy fibre–granule cell synapse of cerebellum during LTP. *J Neurophysiol* **88**, 627–638.

Maffei A, Prestori F, Shibuki K, Rossi P, Taglietti V & D'Angelo E (2003). NO enhances presynaptic currents during cerebellar mossy fibre-granule cell LTP. *J Neurophysiol* **90**, 2478–2483.

Malenka RC & Nicoll RA (1999). Long-term potentiation – A decade of progress? *Science* **285**, 1870–1874.

Malinow R & Tsien RW (1990). Presynaptic enhancement shown by whole-cell recordings of long-term potentiation in hippocampal slices. *Nature* **346**, 177–180.

Mapelli J & D'Angelo E (2007). The spatial organization of long-term synaptic plasticity at the input stage of cerebellum. *J Neurosci* **27**, 1285–1296.

Mapelli L, Rossi P, Nieus T & D'Angelo E (2009). Tonic activation of $GABA_B$ receptors reduces release probability at inhibitory connections in the cerebellar glomerulus. *J Neurophysiol*, **101**, 3089–3099.

Mitchell SJ & Silver RA (2000*a*). Glutamate spillover suppresses inhibition by activating presynaptic mGluRs. *Nature* **404**, 498–502.

Mitchell SJ & Silver RA (2000*b*). GABA spillover from single inhibitory axons suppresses low-frequency excitatory transmission at the cerebellar glomerulus. *J Neurosci* **20**, 8651–8658.

Mulkey RM & Malenka RC (1992). Mechanisms underlying induction of homosynaptic long-term depression in area CA1 of hippocampus. *Neuron* **9**, 967–975.

Nevian T & Sackmann B (2006). Spine Ca^{2+} signalling in spike-timing-dependent plasticity. *J Neurosci* **26**, 11001–11013.

Nieus T, Sola E, Mapelli J, Saftenku E, Rossi P & D'Angelo E (2006). LTP regulates burst initiation and frequency at mossy fibre-granule cell synapses of rat cerebellum: experimental observations and theoretical predictions. *J Neurophysiol* **95**, 686–699.

Nishiyama M, Hong K, Mikoshiba K, Poo MM & Kato K (2000). Ca^{2+} stores regulate the polarity and input specificity of synaptic modification. *Nature* **40**, 584–588.

Oliet SH, Malenka RC & Nicoll RA (1997). Two distinct forms of long-term depression coexist in CA1 hippocampal pyramidal cells. *Neuron* **18**, 969–982.

Prestori F, Rossi P, Bearzatto B, Lainé J, Necchi D, Diwakar S, Schiffmann SN, Axelrad H, & D'Angelo E (2008). Altered neuron excitability and synaptic plasticity in the cerebellar granular layer of juvenile prion protein knock-out mice with impaired motor control. *J Neurosci* **28**, 7091–7103.

Rancz EA, Ishikawa T, Duguid I, Chadderton P, Mahon S & Häusser M (2007). High-fidelity transmission of sensory information by single cerebellar mossy fibre boutons. *Nature* **450**, 1245–1248.

Roggeri L, Rivieccio B, Rossi P & D'Angelo E (2008). Tactile stimulation evokes long-term synaptic plasticity in the granular layer of cerebellum. *J Neurosci* **28**, 6354–6359.

Ronesi J & Lovinger DM (2005). Induction of striatal long-term synaptic depression by moderate frequency activation of cortical afferents in rat. *J Physiol* **562**, 245–256.

Rossi P, Sola E, Taglietti V, Borchardt T, Steigerwald F, Utvik JK, Ottersen OP, Köhr G & D'Angelo E (2002). NMDA receptor 2 (NR2) C-terminal control of NR open probability regulates synaptic transmission and plasticity at a cerebellar synapse. *J Neurosci* **22**, 9687–9697.

Saviane C & Silver RA (2006). Errors in the estimation of the variance: implications for multi-probability fluctuations analysis. *J Neurosci Methods* **153**, 250–260.

Silver RA, Cull-Candy SG & Takahashi T (1996). Non-NMDA glutamate receptor occupancy and open probability at a rat cerebellar synapse with single and multiple release sites. *J Physiol* **494**, 231–250.

Sola E, Prestori F, Rossi P, Taglietti V & D'Angelo E (2004). Increased neurotransmitter release during long-term potentiation at mossy fibre–granule cell synapses in rat cerebellum. *J Physiol* **557**, 843–861.

Stanton PK, Winterer J, Bailey CP, Kyrozis A, Raginov I, Laube G, Veh RW, Nguyen CQ & Müller W (2003). Long-term depression of presynaptic release from the readily releasable vesicle pool induced by NMDA receptor-dependent retrograde nitric oxide. *J Neurosci* **23**, 5936–5944.

van Kan PL, Houk JC & Gibson AR (1993). Output organization of intermediate cerebellum of the monkey. *J Neurophysiol* **69**, 57–73.

Yang SN, Tang YG & Zucker RS (1999). Selective induction of LTP and LTD by postsynaptic $[Ca^{2+}]_i$ elevation. *J Neurophysiol* **81**, 781–787.

Zhang XL, Zhou ZY, Winterer J, Müller W & Stanton PK (2006). NMDA-dependent, but not group I metabotropic glutamate receptor-dependent, long-term depression at Schaffer collateral–CA1 synapses is associated with long-term reduction of release from the rapidly recycling presynaptic vesicle pool. *J Neurosci* **26**, 10270–10280.

Zucker RS (1999). Calcium- and activity-dependent synaptic plasticity. *Curr Opin Neurobiol* **9**, 305–313.

Author contributions

A.D'E. and F.P. contributed equally to experiments, data analysis and paper preparation. E.D'A. participated in experiments and data analysis, and coordinated the whole work and paper writing. The work was carried out in the Laboratory of Neurophysiology, Department of Physiology, University of Pavia.

Acknowledgements

We wish to thank Dr D. Gandolfi and F. Pasquali for helpful contribution to data analysis and acknowledge Dr D. Gall for comments on the manuscript. This work was supported by grants from the European Union (SENSOPAC, FP6-IST028056), Consorzio Interuniversitario per le Scienze Fisiche della Materia (NEUROIMAGE) and Italian Ministry of Research (PRIN-2006059994).